AIAA JOURNAL
Vol. 41, No. 12, December 2003

Compressible Linear Stability of Confluent Wake/Boundary Layers

William W. Liou* and Fengjun Liu†
Western Michigan University Kalamazoo, Michigan 49008

The linear stability of a compressible confluent wake/boundary layer is studied. The base flow model considered is the superposition of a compressible boundary layer and a Gaussian-like wake located above the boundary layer. The linear stability equations have been solved by using a global numerical method. The stability modes of interest have been identified as the boundary-layer modes, the antisymmetric wake mode, and the symmetric wake mode. The effects of wake height on the first Tollmien–Shlichting mode and the second mode associated with the boundary layer are discussed. Results for unstable modes associated with the wake are also presented. At high speeds, in contrast to the incompressible results, a reduced wake height has a strong stabilizing effect on the growth rates of both the first and the second modes associated with the boundary layer. The effects of the reduced wake height on the growth rate of the unstable antisymmetric wake mode vary. For the high-Mach-number case calculated, there exists a frequency for which the growth rate of the unstable antisymmetric mode is neither enhanced nor reduced by the changes in wake height.

Nomenclature

A, B, C	=	coefficient matrices in Eq. (3)
b	=	wake width parameter
C_i	=	imaginary part of wave speed
C_r	=	real part of wave speed
C_0, C_1, C_2	=	coefficient matrices in Eq. (6)
D	=	d/dy
D_2	=	lambda matrix of degree two
F	=	frequency parameter, $\omega^* \bar{\mu}^*_\infty / \bar{\rho}^*_\infty \bar{U}^{*2}_\infty$
h	=	wake height
I	=	identity matrix
i	=	$\sqrt{-1}$
k	=	thermal conductivity
l	=	viscous length scale
M	=	Mach number
N	=	number of grid point in y
P	=	pressure
P_r	=	$\bar{\mu}^*_\infty c_p / \bar{k}^*_\infty$
Re	=	Reynolds number, $\bar{\rho}^*_\infty \bar{U}^*_\infty l / \bar{\mu}^*_\infty$
T	=	base temperature
U	=	base streamwise velocity
u, v, w, p	=	velocity components and pressure
x, y, z	=	streamwise, wall-normal, and spanwise coordinates
α	=	complex streamwise wave number
α_i	=	imaginary part of α
α_r	=	real part of α
β	=	spanwise wave number
ΔU_c	=	wake centerline velocity defect
μ, λ	=	fluid viscosity
ρ	=	density
τ	=	temperature
ϕ	=	eigenfunction
ω	=	frequency

Subscript

∞	=	far field

Superscripts

~	=	instantaneous flow quantity
^	=	eigenfunction
-	=	base flow quantity
*	=	dimensional quantity

Received 24 December 2002; revision received 11 August 2003; accepted for publication 11 August 2003.

*Associate Professor, Department of Mechanical and Aeronautical Engineering. Senior Member AIAA.

†Research Fellow, Department of Mechanical and Aeronautical Engineering. Member AIAA.

I. Introduction

CONFLUENT wake/boundary layers can be observed in the flow around multi-element airfoils in high-lift configurations. They form, for example, on the upper surface of the main element that is located downstream of a slat. In hypersonic scramjet inlets a hypersonic wake/boundary layer flow can form between the cowl trailing-edge wake and the boundary layer in the rear part of the centerbody surface. The confluent wake/boundary layer represents one of the phenomena that are presently not well understood in such flows. Experimental[1–3] and numerical studies based on the averaged Navier–Stokes equations[4,5] and the direct simulation Monte Carlo method[6] have been conducted to better understand the flow physics of the confluent wake/boundary layers. To examine the characteristics of spatially developing small disturbances in incompressible confluent wake/boundary layers, a linear stability analysis has been performed.[7] The effects of the wake height (the distance between the wake centerline and the wall) and the wake velocity defect on the boundary-layer mode and the wake modes were investigated in detail. The incompressible results indicate that the wake above the boundary layer can have an amplifying effect on the growth rate of the boundary-layer mode. The amplifying effect intensifies with reduced wake height and increased wake velocity defect. In addition, the unstable modes associated with the wake were found to be stabilized with reduced wake height.

The work reported here has been performed in an attempt to examine the effect of compressibility on linear stability of confluent wake/boundary layers. Compressibility could be influential to the flow development when the Mach number is high. The existence of a region of high shear in the wake can modify the characteristics of the first and the second modes in high-speed boundary layers and potentially impact the boundary-layer transition. Prediction of the flow transition in boundary layers is of critical importance to high-speed vehicles. Thermal effects resulting from boundary-layer transition represent a critical design constraint for the thermal protection system for all phases of a hypersonic flight.[8]

A detailed theoretical study of the linear stability of compressible flat-plat boundary layers was reported in Lees and Lin.[9] A comprehensive review on this subject can be found in Mack.[10] Multiple modes of stability have been shown to exist in compressible boundary layers. At low Mach number the instability in a compressible boundary layer is of viscous type, and the most amplified disturbances are oblique modes referred to as the first Tollmien–Schlichting (T-S) mode. With an increase of the Mach number, the instability changes to an inviscid type as the generalized inflexion point moves outwards in the boundary layer.[9,10] In addition to the first mode, there exists an infinite sequence of discrete modes that do not require the existence of the generalized inflexion point when the relative freestream Mach number is greater than one.[9] For an insulated flat-plate boundary layer this condition is satisfied[11] at a Mach number of 2.2. The most amplified mode among these discrete modes is normally referred to as the second mode. Mack[10] performed detailed studies of the second mode using a temporal approach. Contrary to the first T-S mode, the second mode waves were found to be generally more unstable and in the form of plane rather than oblique modes. For a hypersonic boundary layer the second mode has higher growth rate than the first mode. The first mode has been shown to be stabilized by surface cooling while the second mode could be destabilized.[11] Linear stability studies[12] for cylinders and cones show that transverse curvature has a destabilizing effect on the first mode and a stabilizing effect on the second mode. The effect of pressure gradient on the stability of compressible boundary layers has been reported by Zurigat et al.[13] The results show that the two-dimensional second mode can be stabilized with favorable pressure gradients and destabilized by adverse pressure gradients.

The stability of compressible wakes has also been extensively studied theoretically[14] and numerically.[15–17] The antisymmetric mode is found to be much more unstable than the symmetric mode over a wide range of frequency.[16] It has been shown that increasing the Mach number results in reduced growth rates for both the antisymmetric and symmetric modes of the wake. An absolute instability can exist in a small region very near the trailing edge of a flat plate for very low Mach number. As the Mach number increases, the absolute instability disappears.[16]

In this paper linear stability theory has been applied to study the spatial stability of compressible confluent wake/boundary layers, which does not appear to have been reported previously. The emphasis here is on the development of the first and the second boundary-layer modes and the wake modes with changes of wake height. In the following, the stability equations are briefly derived. This is followed by a description of base flow profiles and the numerical methods.

II. Technical Approaches

In this section the formulation of the stability problem is presented. The numerical methods used to solve the resulting eigenvalue problem and the assumed base flow model are also described.

A. Compressible Linear Stability Equations

The derivation of the compressible linear stability equations can be readily found in the literature.[9,10,18] It is briefly described here for completeness. The two-dimensional compressible confluent wake/boundary layer with locally parallel base flow is considered in the Cartesian coordinate system (x, y, z) representing the streamwise, the wall-normal, and the spanwise directions, respectively. The spatial scales have been nondimensionalized by a viscous length $l = \sqrt{(\bar{\mu}^*_\infty x^*/\bar{\rho}^*_\infty \bar{U}^*_\infty)}$, pressure by $\bar{\rho}^*_\infty \bar{U}^{*2}_\infty$, and other quantities by their corresponding free stream values $()^*_\infty$, for example, $\bar{U} = \bar{U}^*/\bar{U}^*_\infty$. Instantaneous flow variables $\tilde{\varphi}$ are decomposed into a base and a fluctuation quantity, that is,

$$\begin{aligned} \tilde{u} &= \bar{U} + u, \qquad \tilde{v} = v, \qquad \tilde{w} = w \\ \tilde{p} &= \bar{P} + p, \qquad \tilde{\tau} = \bar{T} + T, \qquad \tilde{\rho} = \bar{\rho} + \rho \\ \tilde{\mu} &= \bar{\mu} + \mu, \qquad \tilde{\lambda} = \bar{\lambda} + \lambda, \qquad \tilde{k} = \bar{k} + k \end{aligned} \tag{1}$$

Separable solutions in the normal mode form are sought for the disturbances:

$$(u, v, w, p, T) = [\hat{u}(y), \hat{v}(y), \hat{w}(y), \hat{p}(y), \hat{T}(y)]e^{i(\alpha x + \beta z - \omega t)} \tag{2}$$

For the spatial stability considered here, α is complex, and ω is real. As a result, the linearized equations for the fluctuations lead to the following system of ordinary differential equations[18]:

$$(AD^2 + BD + C)\phi = 0 \tag{3}$$

where $\phi = (\hat{u}, \hat{v}, \hat{p}, \hat{T}, \hat{w})^{Tr}$ and A, B, and C are 5×5 coefficient matrices. The details of coefficient matrices can be found, for example, in Malik[18] and are not given here. The boundary conditions can be written as

$$\hat{u}, \hat{v}, \hat{T}, \hat{w} = 0 \quad \text{at} \quad y = 0; \qquad \hat{u}, \hat{v}, \hat{T}, \hat{w} \to 0 \quad \text{at} \quad y \to \infty \tag{4}$$

The pressure at both the solid wall and the freestream can be obtained by evaluating the normal momentum equation. Sutherland's law has been used for $\tilde{\mu}$ and $\tilde{\lambda} = -\frac{2}{3}\tilde{\mu}$. The Prandtl number P_r is set at 0.7.

B. Numerical Methods

Sixth-order-accurate finite differencing has been applied to discretize Eq. (3). The finite difference formulas can be readily derived using the Taylor-series expansion. A grid-stretching method[7] has been employed to generate the grid node distribution in the physical domain. The grid stretching allows for higher node density in the high shear regions near the wall and in the wake.

The discretization of Eq. (3) using the sixth-order finite difference method results in a system of homogeneous equations nonlinear in the parameter α:

$$D_2(\alpha)\{\phi\} = 0 \tag{5}$$

The matrix $D_2(\alpha)$ is a lambda matrix of degree two and can be expressed as a scalar polynomial with matrix coefficients:

$$D_2(\alpha) = C_0\alpha^2 + C_1\alpha + C_2 \tag{6}$$

The matrices C_i are square matrices of order $5N$. A linear companion matrix method[19] has been used to solve Eq. (5). The detailed procedure can be found in Bridges and Morris.[19] A local iteration method[19] has been used to find the eigenfunctions. This procedure is very effective, and convergence is usually obtained in two to three iterations using the unit vector as an initial guess.

C. Base Flow Model

The flow model adopted here is composed of two separate regions where flow gradients can occur. They are the region near the wall where the compressible boundary layer develops and the region away from the wall where the wake generated by, presumably, a body upstream is located. As has been mentioned earlier, the base flow is assumed to be two-dimensional and locally parallel. For the boundary layer the velocity and the temperature profiles can be obtained by solving the following similarity equations[20]:

$$(cf'')' + ff'' = 0 \tag{7}$$

$$(a_1 g' + a_2 f' f'')' + fg' = 0 \tag{8}$$

where

$$f' \equiv \bar{U}, \quad g \equiv \bar{H}, \quad c \equiv \bar{\rho}\bar{\mu}$$

$$a_1 \equiv \frac{c}{P_r}, \quad a_2 = \frac{(\gamma - 1)M^2}{1 + (\gamma - 1/2)M^2}\left(1 - \frac{1}{P_r}\right)c \tag{9}$$

Equations (7–9) have been solved by using fourth-order finite differencing. Adiabatic wall conditions are specified. For the velocity profile in the wake region, a Gaussian-like function has been assumed:

$$\bar{U} = 1.0 - \Delta U_c \exp[-b(y - h)^2] \tag{10}$$

For all of the cases calculated in the present study, the velocity defect ΔU_c and the width parameter b have been set at 0.6915 and 0.69315, respectively, which is used in Sato and Kariki.[21] The Crocco–Busemann relation has been employed to obtain the temperature profile in the wake. That is,

$$\bar{T} = 1.0 + 0.5M^2(\gamma - 1)(1 - \bar{U}^2) \tag{11}$$

The velocity and temperature distributions associated with the confluent wake/boundary layer are assumed to be linear superpositions of the corresponding profiles for the wake and the boundary layer just described. Figure 1 shows the resulting profiles of velocity and temperature for a modeled compressible confluent wake/boundary layer with $M = 4.5$, $h = 50$, and a Reynolds number of 1500.

III. Results and Discussion

This section begins with a presentation of the results of numerical tool validation, which includes Tables 1 and 2 as well as Figs. 2 and 3. The validated numerical solver is then applied to examine the characteristics of the stability modes in compressible confluent wake/boundary layers.

A global solver has been developed in this study to solve the eigenvalue problem associated with the spatial linear stability analysis. It solves for the eigenvalue spectrum with a prescribed spanwise wave number β and a frequency ω. The solver has been validated by examining the stability results for the Blasius boundary layer and compressible boundary layers, respectively. Table 1 shows a comparison of the calculated eigenvalue α for the Blasius boundary layer with published results[7,22,23] for different values of ω, β, and Reynolds number Re. The number of grid nodes is 101, and the Mach number is set at 10^{-5}. The present values agree well with the various cited published results. Table 2 shows a comparison of the validation results for compressible boundary layers.[18,24,25] Flows of two different Mach numbers have been calculated for different values of frequency and spanwise wave number. The velocity and the temperature profiles of the base flow have been obtained by solving Eq. (7) and (8). The data of Malik[18] was obtained by using a multidomain spectral collocation method. Chang[24] used a finite difference method, and a spectral collocation method was applied in Liou and Fang.[25] Table 2 shows that the calculated eigenvalues compare well with the results obtained by using the various other numerical discretization methods. This is true for the plane as well as the oblique modes.

Figure 2 compares the calculated variation of the unstable mode growth rate with the Reynolds number for the boundary layers studied in Zurigat et al.[13] The Mach numbers are 0.0 and 1.0. The frequency parameter F is 45×10^{-6}. The results indicate that the present values are in a very good agreement with those of Zurigat et al.[13] For a high-speed boundary layer[13] with $M = 4.5$, $Re = 1500$, and $\bar{T}^*_\infty = 120$ K, Fig. 3 shows a comparison of the changes of the growth rate with frequency for the two-dimensional second modes

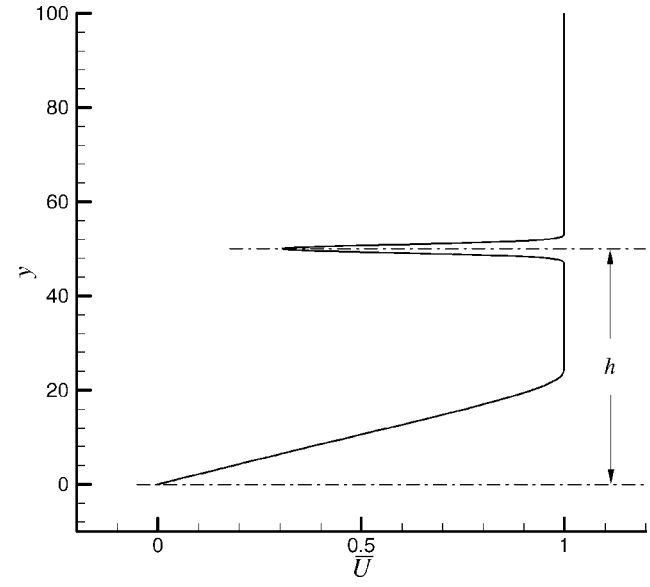

a) Velocity

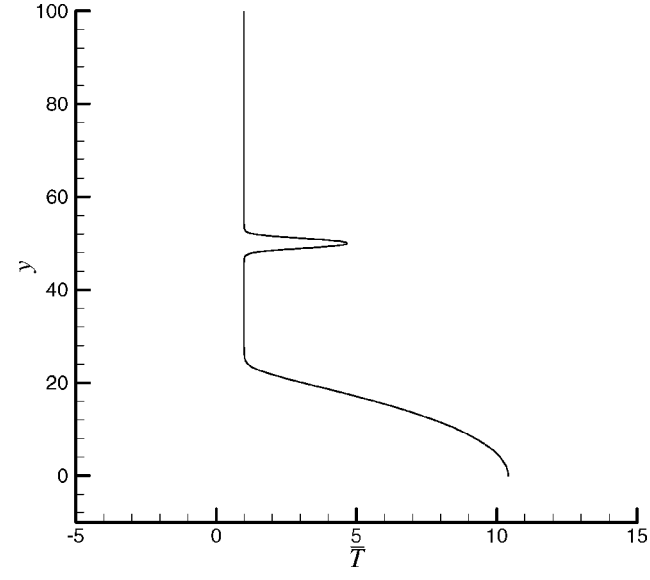

b) Temperature

Fig. 1 Base flow profiles for the CCWB: $M = 4.5$ and $Re = 1500$.

Table 1 Eigenvalue comparison for the Blasius boundary layer

Re	ω	β	Reference	Present
3.36×10^2	0.1297	0.00	$0.30840 + i0.0079$ (Ref. 22)	$0.308350 + i0.007939$
5.98×10^2	0.1201	0.00	$0.30790 - i0.0019$ (Ref. 22)	$0.307850 - i0.001897$
9.98×10^2	0.1122	0.00	$0.30860 - i0.0057$ (Ref. 22)	$0.308591 - i0.005708$
1.0×10^3	0.0700	0.12	$0.19861 - i0.0042$ (Ref. 23)	$0.198610 - i0.004202$
1.5×10^3	0.0900	0.00	$0.268656 - i0.009349$ (Ref. 7)	$0.268656 - i0.009349$

Table 2 Eigenvalue comparison for compressible boundary layers: Re = 1500

M	ω	β	Reference	Present
4.5[a]	0.23	0.00	$0.2534048 - i0.0024921$ (Ref. 18)	$0.253402 - i0.0024902$
4.5[a]	0.23	0.00	$0.2534690 - i0.0024949$ (Ref. 24)	$0.253402 - i0.0024902$
5.0[b]	0.17	0.00	$0.186935 - i0.002693$ (Ref. 25)	$0.186937 - i0.002690$
5.0[b]	0.17	0.10	$0.184940 - i0.001466$ (Ref. 25)	$0.184939 - i0.001464$

[a] $\bar{T}^*_\infty = 120$ K, [b] $\bar{T}^*_\infty = 50$ K.

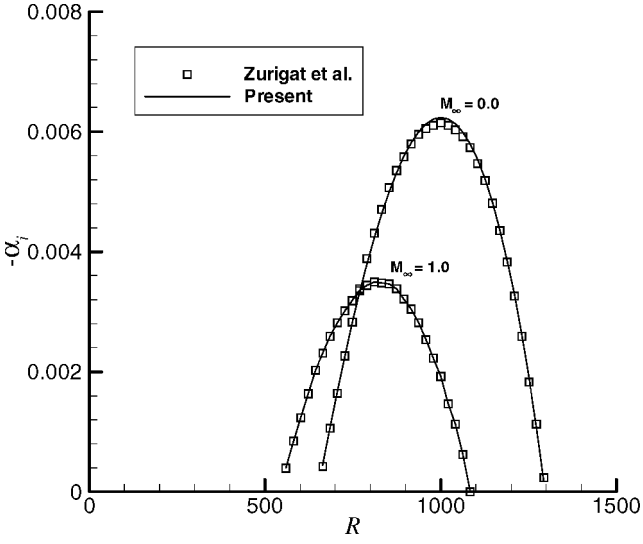

Fig. 2 Variation of unstable mode growth rate with Reynolds number: $F = 45 \times 10^{-6}$.

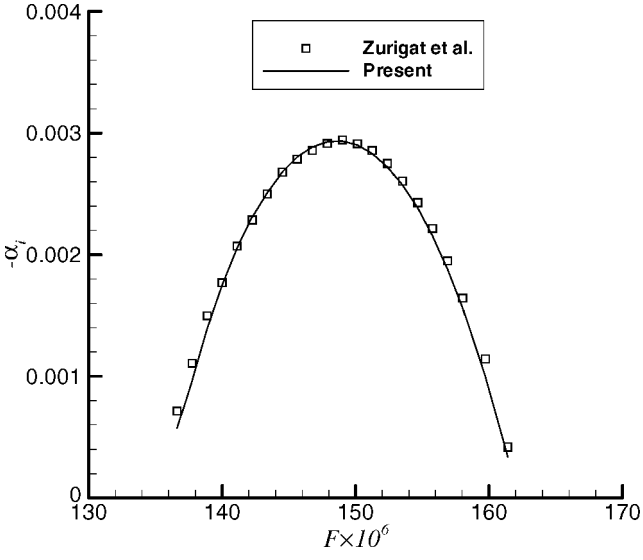

Fig. 3 Variation of the growth rate of the two-dimensional second modes: $M = 4.5$ and $Re = 1500$.

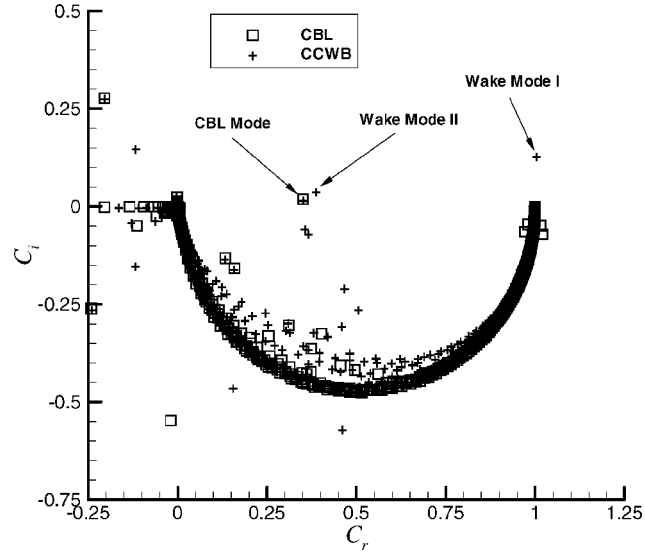

Fig. 4 Wave speed spectra for the CBL and CCWB: $M = 1.0$, $Re = 1500$, $\omega = 0.027$, $\beta = 0.05$, and $h = 60$.

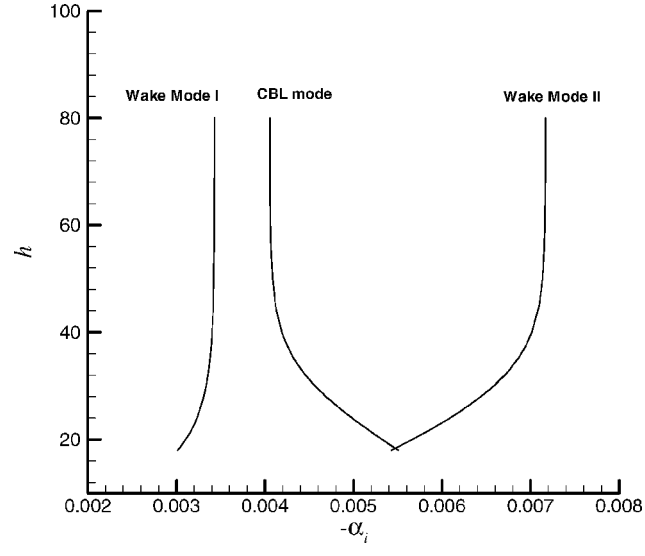

Fig. 5 Growth rates for various modes: $M = 1.0$, $Re = 1500$, $\omega = 0.027$, and $\beta = 0.05$.

($\beta = 0$). The agreement between the present results and that of Zurigat et al.[13] appears to be quite satisfactory. The results of the code validation show that the solver developed is an accurate numerical tool. In the following, the linear stability results obtained by using the validated numerical solver for compressible confluent wake/boundary layers (CCWB) are presented.

Figure 4 shows the wave speed (ω/α) spectra for a compressible boundary layer (CBL) and a CCWB for $M = 1.0$, $Re = 1500$ and $\bar{T}^*_\infty = 120$ K. The distance between the centerline of the wake and the wall $h = 60$. The spectra are shown for a frequency $\omega = 0.027$ and a spanwise wave number $\beta = 0.05$. For the given Reynolds number and Mach number they represent the first boundary-layer mode in the CBL. The first mode associated with the boundary layer has been determined by enforcing the condition $d\alpha_i/d\beta = 0$. The computations have been performed on a stretched grid $N = 251$, with nodes clustering in the wake and near the wall. The smallest and the largest grid spacing are 0.072517 and 0.97, respectively. Grid-independence studies indicate that the solutions remain unchanged for grids with more nodes. Interactions between the wake and the boundary layer at such a large separation are expected to be negligible. As shown in Fig. 4, a discrete mode in the CCWB spectrum collapses onto the first mode of the CBL and thus can be identified as the first mode associated with the boundary layer. In addition to the boundary-layer mode, two other discrete modes found in the CCWB spectrum have also been identified as the antisymmetric and symmetric modes associated with the wake. The antisymmetric and the symmetric modes, determined according to their streamwise velocity perturbation distributions,[16] will be referred to as wake mode I and wake mode II, respectively. There is also a collapse of the continuous parts[26] of the CBL and the CCWB spectra. Because $C_i > 0$ for the boundary-layer mode and wake modes I and II, they are spatially unstable and are of interest in this paper.

Figure 5 shows the variation of the growth rates for the boundary-layer mode, wake mode I, and wake mode II with the wake height h for $M = 1.0$, $Re = 1500$, $\omega = 0.027$, and $\beta = 0.05$. As the wake moves toward the wall (decreasing in h), the first mode associated with the boundary layer is found to be amplified while the wake modes are damped. Similar patterns of the growth rate variation with h have been reported[7] for incompressible confluent wake/boundary layers. The results indicate that for the CCWB of $M = 1.0$ the stability modes exhibit an incompressible-like behavior. That is, the presence of wake can enhance the disturbance growth in the boundary layer. On the other hand, the disturbance growth in the wake can be reduced.

Figure 6 shows the effects of the Mach number ($M = 1.0 \sim 4.5$) on the growth rate of the first mode associated with the boundary

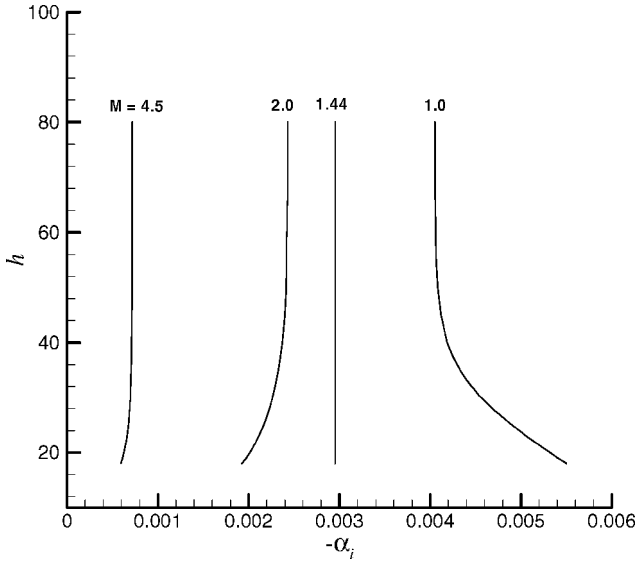

Fig. 6 Growth rates for the first mode: $Re = 1500$.

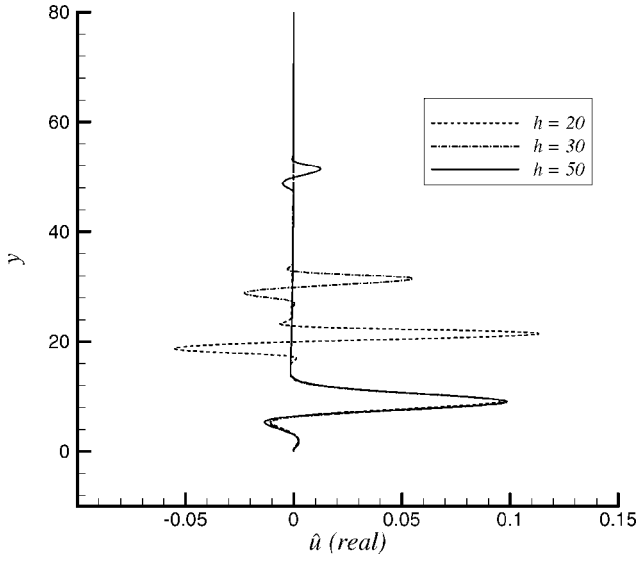

Fig. 8 Mode shapes for the disturbance streamwise velocity component (first mode): $M = 4.5$, $Re = 1500$, $\omega = 0.0275$, and $\beta = 0.076$.

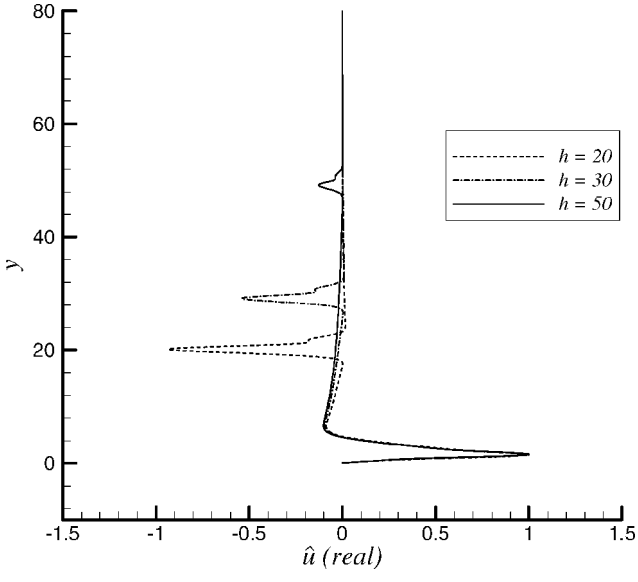

Fig. 7 Mode shapes for the disturbance streamwise velocity component (first mode): $M = 1.0$, $Re = 1500$, $\omega = 0.027$, and $\beta = 0.05$.

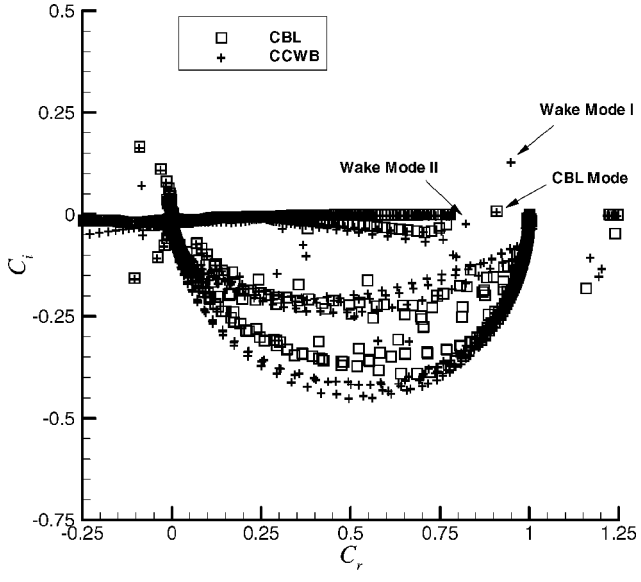

Fig. 9 Wave speed spectra for the CBL and CCWB: $M = 4.5$, $Re = 1500$, $\omega = 0.23$, $\beta = 0$, and $h = 60$.

layer as the wake height changes. The velocity and temperature distributions of the base flow for $M = 4.5$ and $h = 50$ have been shown in Fig. 1. The first mode is stabilized with an increase of Mach number, as has been reported in many previous compressible boundary-layer stability studies. Figure 6 also shows that the effect of the wake height on the first mode growth rate reverses with the increasing Mach number: from being amplified at low Mach numbers to being damped at high Mach numbers. For $Re = 1500$, this reversal of amplification occurs at a Mach number of 1.44. That is, for the CCWB with a freestream Mach number of 1.44 the growth rate of the first mode is independent of the wake height calculated. The damping effect at high Mach numbers appears to lessen with further increase of Mach number.

Figures 7 and 8 show the real parts of the mode shapes of the disturbance streamwise velocity component u of the boundary-layer first mode for the CCWB with $M = 1.0$ and 4.5, respectively. They have been normalized by their respective maximum values in the eigenfunction ϕ. When the wake is brought close to the wall, it has a significant effect on the mode shapes of the first mode in the wake region and little effect in the boundary-layer region for both Mach numbers. This insensitivity of mode shapes in the wall region to wake height has also been observed in incompressible confluent wake/boundary layers.[7] The profiles of the boundary-layer mode shape in the region of the wake are nearly symmetric for $M = 1.0$ (Fig. 7) and antisymmetric for $M = 4.5$ (Fig. 8). This behavior of the mode shapes in the wake region agrees with the fact that, with $\omega = 0.027$, the dominant wake mode is symmetric at $M = 1$ and antisymmetric at $M = 4.5$.

At high Mach number the second mode has been found to be the dominant boundary-layer mode. The second mode calculations have been performed by setting $\beta = 0$, which gives the highest growth rates. Figure 9 shows the wave speed spectra for a CCWB with $h = 60$ and a CBL of the same Mach number ($= 4.5$). The frequency is 0.23. The CBL mode indicated in Fig. 9 represents the second mode associated with the boundary layer, which can also be found in the eigenvalue spectrum for the CCWB. Wake mode I and wake mode II can be identified in the CCWB spectrum by examining their mode shapes.

Figure 10 shows the variations of the growth rate of the second mode with wake height for different Reynolds numbers (750, 1500 and 3000) and a Mach number of 4.5. The damping effect of the reduced wake height on the growth rate of the second mode associated

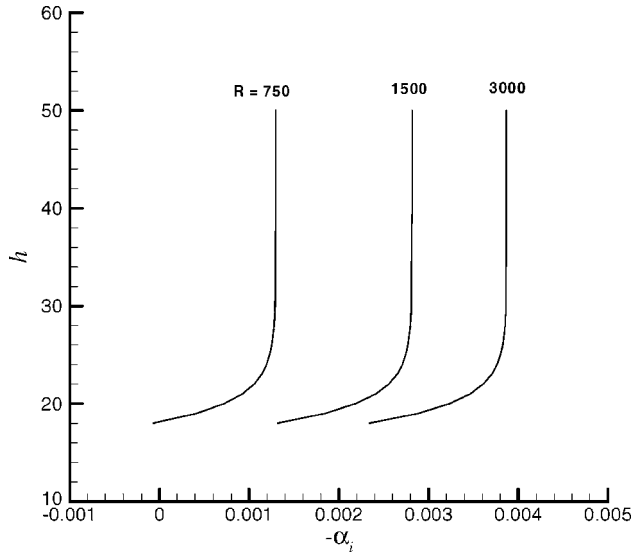

Fig. 10 Growth rates of the two-dimensional second modes: $M = 4.5$.

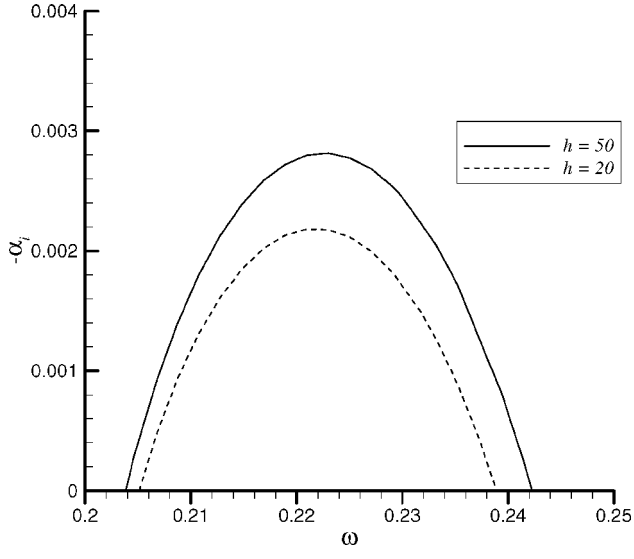

Fig. 11 Growth rates of the two-dimensional second modes: $M = 4.5$ and $Re = 1500$.

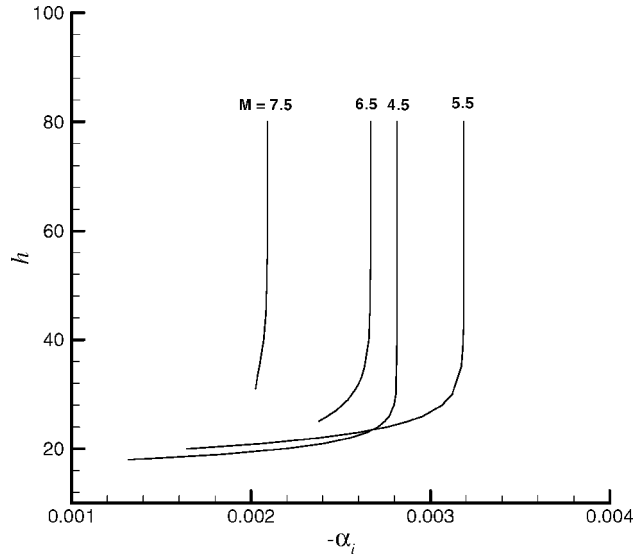

Fig. 12 Growth rates of the second mode: $Re = 1500$.

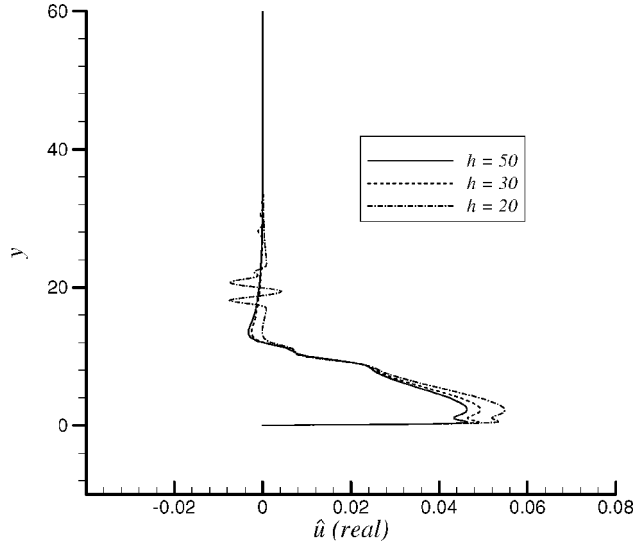

Fig. 13 Mode shapes for the disturbance streamwise velocity component (second mode): $M = 4.5$, $Re = 1500$, $\omega = 0.2225$, and $\beta = 0$.

with the boundary layer is more apparent for cases with wakes closer to the wall. This damping of the second mode with reduced wake height exists for all three Reynolds numbers calculated.

Figure 11 shows the influence of wake height on the growth rate of the boundary-layer mode for a range of frequency for $h = 20$ and 50. The decrease of growth rate with the reduced wake height is apparent for the entire range of frequency calculated.

Figure 12 shows the effect of wake height on the growth rate of the second mode for four different Mach numbers ($4.5 \sim 7.5$) and $Re = 1500$. Because the boundary-layer thickness tends to increase as the Mach number increases, the minimum wake height for the nonmerging base flow model for CCWB adopted here to be valid also increases with Mach number. The damping effect of wake on the second mode observed in Fig. 10 is apparent for all of the Mach numbers calculated. Note that the reversed trend of variation of the growth rate of the second mode with increasing Mach number observed for the CCWB with large value of h, say, for $h = 80$, is consistent with that for CBL reported in Mack.[10]

The real parts of the mode shapes for u for the second mode are presented in Fig. 13 for three different wake heights ($h = 20$, 30, and 50), where $M = 4.5$, $Re = 1500$ and $\omega = 0.2225$. In comparison with the mode shapes shown in Fig. 8 for the first mode, the mode shape variation with wake height for the second mode is more apparent in the boundary-layer region. In the regions where the wakes are located, the distributions are nearly symmetric. The amplitudes, relative to their peak levels in the boundary-layer region, are also smaller than those shown in Fig. 8 for the first mode.

Figure 14 shows the variations of the growth rate of wake mode I with the wake height for three different Reynolds numbers and for a Mach number of 4.5. The frequencies are 0.2185, 0.2225, and 0.226 for the Reynolds numbers of 750, 1500, and 3000, respectively. They are associated with the second mode of the boundary layer. Wake mode I is dampened with the reduced wake height for the three Reynolds numbers calculated. The wall damping effect decreases with the increase of the Reynolds number, indicating a viscous mechanism at play with the varying wake height.

Figure 15 shows the variation of the growth rate of wake mode I for two high-speed CCWB with $M = 4.5$ and 7.5, respectively, and for $h = 20$, 27, and 50. There is an apparent decrease of the growth rate with Mach number in the frequency range calculated. Except for near the neutral frequencies, the growth rate of wake mode I for $M = 4.5$ is rather insensitive to changes in wake height. At the high Mach number of 7.5, the effect of wake height on the growth rate appears to change from causing a small amount of damping to amplifying as the frequency increases from the lower neutral frequency. The frequency at which the effect of wake height reverses

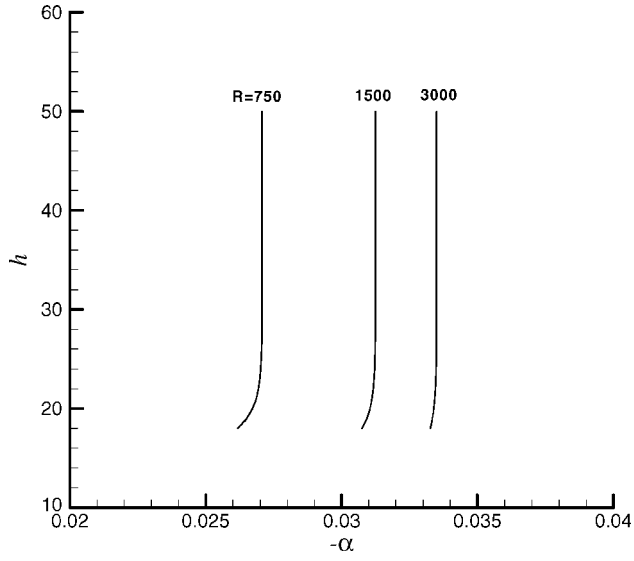

Fig. 14 Variation of the growth rate for wake mode I: $M = 4.5$.

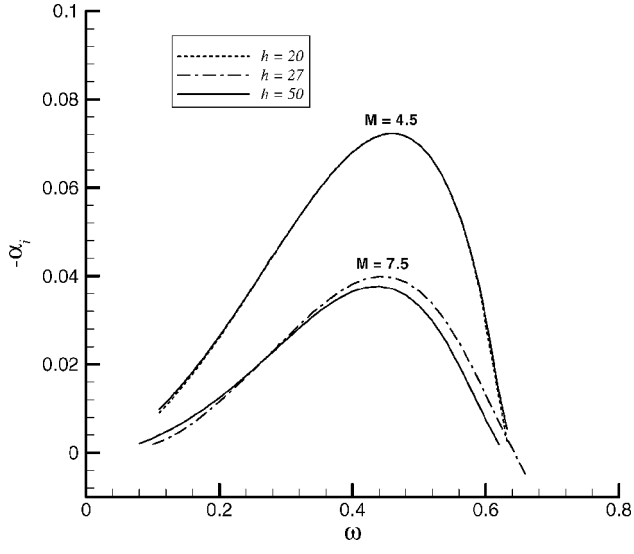

Fig. 15 Variation of the growth rate for wake mode I with frequency: $Re = 1500$ and $\beta = 0$.

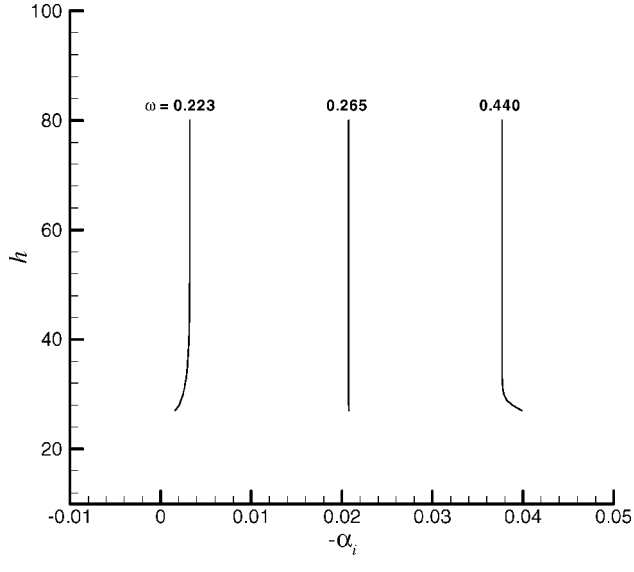

Fig. 16 Growth rate variation for wake mode I: $M = 7.5$, $Re = 1500$ and $\beta = 0$.

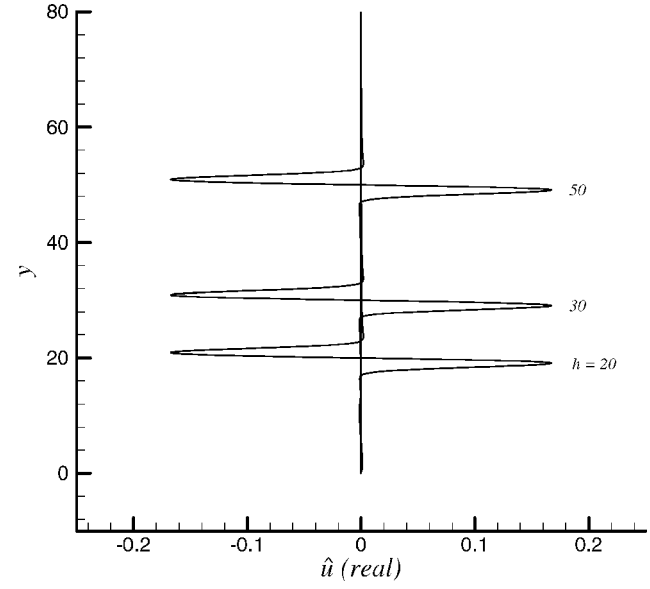

Fig. 17 Mode shapes for the disturbance streamwise velocity component (wake mode I): $M = 4.5$, $Re = 1500$, $\omega = 0.2225$, and $\beta = 0$.

is found to be about 0.265. Calculations at other wake heights were then performed. The results show that the frequency at which this reversal occurs is independent of wake height for the present case of $M = 7.5$. Figure 16 shows the variation of the growth rate for three frequencies, including that for $\omega = 0.265$ and two others located on either sides of the reverse frequency.

Figure 17 shows the real parts of the mode shapes for u of wake mode I for $M = 4.5$, $Re = 1500$, and $\omega = 0.2225$. Wake mode I is an antisymmetric mode, which can be clearly seen in the mode-shape distributions. The mode shape for the disturbance mode associated with the wake is negligibly small in the near-wall region compared with that in the wake region and remains so for all of the three wake heights calculated. In the wake region the mode shapes of wake mode I do not change significantly other than apparent translations of profiles with the wake locations.

IV. Summary

Spatial linear stability of compressible confluent wake/boundary layers has been studied using a global numerical method. Various stability modes have been identified. At low Mach numbers the first mode associated with the boundary layer and the wake modes has been shown to vary in a manner similar to those of incompressible confluent wake/boundary layers. That is, reduced wake height tends to cause the growth rate of the boundary-layer mode to increase and those of the wake modes to decrease. As the Mach number increases, the effect of reduced wake height on the first boundary-layer mode changes from amplifying to damping. For the cases calculated, this reversal of wake-height effect occurs at a Mach number of 1.44. The second mode associated with the boundary layer has also been found to be dampened with decreases in wake height. For the antisymmetric unstable wake mode there are apparent translations of the mode shapes with the wake locations. The effect of the wake height on the growth rate is small but appears to be frequency-dependent at high Mach number.

The dampening effect of the wake on the growth rates of the boundary-layer modes at high speeds suggests that the linear growth of small disturbances can be lessened and lead to a delay of the occurrence of transition in the boundary layer. For multi-element airfoils and scramjet engines, where high-speed confluent wake/boundary-layer flows appear, the impact of such changes of flow characteristics on the aerodynamic design can be important.

References

[1] Bario, F., Charnay, G., and Papailiou, K. D., "An Experiment Concerning the Confluence of a Wake and a Boundary Layer," *Journal of Fluids Engineering*, Vol. 104, No. 3, 1982, pp. 18–24.

[2]Thomas, F. O., Nelson, R. C., and Liu, X., "Experimental Investigation of the Confluent Boundary Layer of a High-Lift System," *AIAA Journal*, Vol. 36, No. 6, 2000, pp. 978–988.

[3]Minucci, M. A. S., and Nagamatsu, H. T., "Investigation of a Two-Dimensional Scramjet Inlet, $M_\infty = 8$-18 and $T_0 = 4100$ K," *Journal of Propulsion and Power*, Vol. 9, No. 1, 1993, pp. 139–145.

[4]Liou, W. W., and Liu, F., "Computational Modeling for the Transitional Flow over a Multi-Element Airfoil," AIAA Paper 2000-4322, 2000.

[5]Rumsey, C. L., Thomas, B. G., Ying, S. X., and Bertelrud, A., "Prediction of High-Lift Flows Using Turbulent Closure Models," *AIAA Journal*, Vol. 36, No. 5, 1998, pp. 765–774.

[6]Chung, C. H., Kim, S. C., Witt, K. J. D., and Nagamatsu, H. T., "Numerical Analysis of Hypersonic Low-Density Scramjet Inlet Flow," *Journal of Spacecraft and Rockets*, Vol. 32, No. 1, 1995, pp. 60–66.

[7]Liou, W. W., and Liu, F. J., "Spatial Linear Instability of Confluent Wake/Boundary Layers," *AIAA Journal*, Vol. 11, No. 11, 2001, pp. 2076–2081.

[8]Wuester, K. E., "An Assessment of the Impact of Transition on Advanced Winged Entry Vehicle Termal Protection System Mass," AIAA Paper 81-0019, 1981.

[9]Lees, L., and Lin, C. C., "Investigation of the Stability of the Laminar Boundary Layer in a Compressible Fluid," NACA TN 1115, Sept. 1946.

[10]Mack, L. M., "Boundary Layer Linear Stability Theory," AGARD, Rept. 709, March 1984.

[11]Malik, M. R., "Prediction and Control of Transition in Supersonic and Hypersonic Boundary Layers," *AIAA Journal*, Vol. 27, No. 11, 1989, pp. 1487–1493.

[12]Spall, R. E., and Malik, M. R., "Effect of Transverse Curvature on the Stability of Compressible Boundary Layers," *AIAA Journal*, Vol. 29, No. 10, 1991, pp. 1596–1602.

[13]Zurigat, Y. H., Nayfeh, A. H., and Masad, J. A., "Effect of Pressure Gradient on the Stability of Compressible Boundary Layers," *AIAA Journal*, Vol. 30, No. 9, 1992, pp. 2204–2211.

[14]Lees, L., and Gold, H., "Stability of Laminar Boundary Layers and Wakes at Hypersonic Speeds, Part I. Stability of Laminar Wakes," *Proceedings of the International Symposium on Fundamental Phenomena in Hypersonic Flow*, Cornell Univ. Press, Ithaca, NY, 1966, p. 130.

[15]Chen, J. H., "The Effect of Mach Number on the Stability of a Plane Supersonic Wake," *Physics of Fluids A*, Vol. 2, No. 6, 1990, pp. 984–1004.

[16]Papageorgiou, D. T., "Linear Instability of the Supersonic Wake Behind a Flat Plate Aligned with a Uniform Stream," *Theoretical and Computational Fluid Dynamics*, Vol. 1, 1990, pp. 327–348.

[17]Papageorgiou, D. T., "The Stability of Two-Dimensional Wakes and Shear Layers at High Mach Numbers," *Physics of Fluids A*, Vol. 3, No. 5, 1991, pp. 793–802.

[18]Malik, M. R., "Numerical Methods for Hypersonic Boundary Layers Stability," *Journal of Computational Physics*, Vol. 86, 1990, pp. 376–413.

[19]Bridges, T. J., and Morris, P. J., "Differential Eigenvalue Problems in Which the Parameter Appears Nonlinearly," *Journal of Computational Physics*, Vol. 55, 1983, pp. 437–463.

[20]Cebeci, T., and Smith, A. M. O., *Analysis of Turbulent Boundary Layers*, Academic Press, New York, 1974.

[21]Sato, H., and Kariki, K., "The Mechanism of Transition in the Wake of a Thin Flat Plate Placed Parallel to a Uniform Flow," *Journal of Fluid Mechanics*, Vol. 11, 1961, pp. 321–352.

[22]Jordinson, R., "The Flat Plate Boundary Layer. Part 1. Numerical Integration of the Orr–Sommerfeld Equation," *Journal of Fluid Mechanics*, Vol. 43, No. 4, 1970, pp. 801–811.

[23]Bridges, T. J., and Morris, P. J., "Boundary Layer Stability Calculations," *Physics of Fluids*, Vol. 30, No. 11, 1987, pp. 3351–3358.

[24]Chang, C.-L., "The Langley Stability and Transition Analysis Codes(LASTRAC)–LST, Linear & Nonlinear PSE for 2D, Axisymmetric and Infinite Swept Wing Boundary Layers," AIAA Paper 2002-0974, 2002.

[25]Liou, W. W., and Fang, Y., "Bursting Frequency Predictions for Compressible Turbulent Boundary Layers," *AIAA Journal*, Vol. 41, No. 6, 2003, pp. 1022–1028.

[26]Balakumar, P., and Malik, M. R., "Discrete Modes and Continuous Spectra in Supersonic Boundary Layers," *Journal of Fluid Mechanics*, Vol. 239, 1992, pp. 631–656.

A. Karagozian
Associate Editor